LXXXI ESNT WORKSHOP «*Light nuclei between single-particle and clustering features*»

Spectrum and EM properties in a macroscopic α-cluster model for ^{24}Mg:

Evidence of $\mathcal{D}_{4h}$ symmetry

5th December 2024

Light Nuclei Workshop
CEA Paris-Saclay
2024

Gianluca Stellin and Karl-Heinz Speidel

CEA Paris-Saclay, ESNT & DRF/DPhN/IRFU/LENA

Macroscopic α-cluster models

Phenomenological approaches, describing **even-even self-conjugate** nuclei in terms of interacting *α-particles* as the only degrees of freedom. Pioneers: Wheeler (1937), Wefelmeier (1937), Hafstad and Teller (1938).

Applications:

α-α scattering: *Nucl. Phys.* **80**, 99-112 (1966), …

^{8}Be: *Phys. Rev.* **59**, 27-36 (1941), *Prog. in Part. and Nucl. Phys.* ***110***, 103735 (2020), …

^{12}C: *Phys. Rev.* **103**, 701 (1956), *Zeitschr. f. Phys.* **290**, 93-105 (1979), *Phys. Rev. C* **61**, 067305 (2000), *Ann. of Phys.* **298**, 344-360 (2002), *J. of Phys. G* **43**, 024003 (2016), *J. of Phys. G* **43**, 085104 (2016), *Few-Body Syst.* **58**, 19 (2017), *Prog. in Part. and Nucl. Phys.* ***110***, 103735 (2020), *Phys. Rev. C* **102**, 014314 (2020), …

^{16}O: *Phys. Rev.* **57**, 454 (1940), *Nucl. Phys. A* **165**, 199-210 (1971), *Few-Body Syst.* **38**, 97-101 (2006), *Phys. Rev. Lett.* **112**, 152501 (2014), *Nucl. Phys. A* **957**, 154-176 (2017), *Prog. in Part. and Nucl. Phys.* ***110***, 103735 (2020), *Phys. Rev. C* **102**, 014314 (2020), …

^{20}Ne: *Phys. Rev.* **152**, 1023 (1966), *Phys. Rev. C* **4**, 1044 (1971), *Nucl. Phys. A* **1006**, 122077 (2021), ...

^{24}Mg: *Phys. Rev.* **152**, 1023 (1966), *Phys. Rev. C* **4**, 1044 (1971), …

^{28}Si: *Phys. Rev.* **145**, 727 (1966), *Phys. Rev. C* **4**, 1044 (1971), …

^{32}S: *Phys. Rev.* **145**, 727 (1966), *Phys. Rev. C* **4**, 1044 (1971), …

^{36}Ar: *Phys. Rev. C* **4**, 1044 (1971), …

« Becoming conglomerates of a small number of α-particles, nuclei acquire *molecular shapes*, differing markedly from the ones of quadrupole (prolate or oblate) or octupole (pear-shaped) type, which originate from the deformation a continuous spherical surface. The associated finite discrete-symmetries are referred to as ***exotic nuclear symmetries***»

I. Dedes, J. Dudek et al. ***SSNET '24***

Consequence: ^{16}O (tedrahedron $\rightsquigarrow \mathcal{T}_d$ symmetry): $\mathscr{I}_x = \mathscr{I}_y = \mathscr{I}_z$ *It has rotational bands!*

Geometric α-cluster model

In this macroscopic approach (**GαCM**), the N α-partcles rotate and vibrate about their equilibrium positions, sitting at the vertices of a *polyhedral structure*. Equilibrium configurations are characterized by a *point symmetry group* $\mathcal{G}$, whereas $\mathcal{G}(\mathrm{N})$ is the *permutation-inversion group* of the N α-partcles.

Equilibrium α-structures for ^{24}Mg (N=6):

linear chain $\mathcal{C}_{\infty v}$

$n_b \equiv$ number of nearest-neighbour bonds $= 5$

✗ Superdeformed prolate

✗ has the lowest n_b

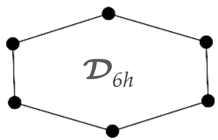

$\mathcal{D}_{6h}$

hexagon

$n_b = 6$

✗ Superdeformed oblate

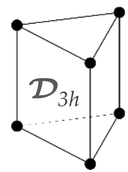

$\mathcal{D}_{3h}$

triangular prism

$n_b = 9$

● quite low n_b

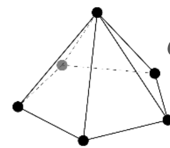

$\mathcal{C}_{5v}$

pentagonal pyramid

$n_b = 10$

✗ absence of inversion symmetry

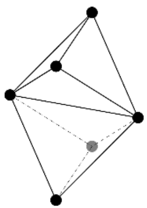

$\mathcal{D}_{2h}$

bitetrahedron

$n_b = 11$

● triaxial

✗ 0^- levels expected

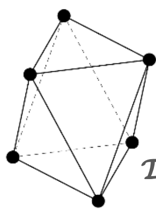

$\mathcal{D}_{3d}$

triangular antiprism

$n_b = 12$

● absence of inversion symmetry

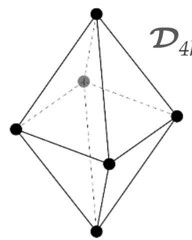

$\mathcal{D}_{4h}$

square bipyramid

$n_b = 12$

✓ **our ansatz**

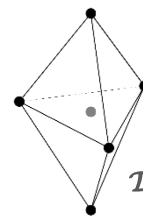

$\mathcal{D}_{3h}$

triangular bipyramid

$n_b = 14$

✓ largest n_b

● more suitable for oblate shapes

► *Inspiration*: R. Bijker and F. Iachello, *Nucl. Phys. A* **1006**, 122077 (2021)

The rotational-vibrational hamiltonian

- The system is described the quantum vibration-rotation Hamiltonian, with N = 6 α-clusters:

$$H = \frac{1}{2}\sum_{\alpha\beta}(J_\alpha - p_\alpha)\mu_{\alpha\beta}(J_\beta - p_\beta) + \frac{1}{2}\sum_{j=1}^{3N-6} P_j^2 + \frac{1}{2}\sum_{j=1}^{3N-6}\lambda_j Q_j^2 - \frac{\hbar^2}{8}\sum_\alpha \mu_{\alpha\alpha}$$

i.e. the GαCM Hamiltonian

⇝ J.K.G. Watson, *Mol. Phys.* **15**, 479-490 (1968)

where:

- $Q_1,\ Q_2\ \dots\ Q_{3N-6}$ are the *normal* vibrational coordinates, and $P_j = -i\hbar\frac{\partial}{\partial Q_j}$ the conjugate momenta $j = 1, 2 \dots 3N-6$
- $\boldsymbol{\mu}$ is the *effective* reciprocal inertia tensor: $\mu^{-1}_{\alpha\beta} = I_{\alpha\beta} - \sum_{k=1}^{3N-6}\left(\sum_{j=1}^{3N-6}\zeta^\alpha_{jk}Q_j\sum_{l=1}^{3N-6}\zeta^\beta_{lk}Q_l\right)$

inertia tensor

where $\zeta^\gamma_{jk} \equiv \sum_{\alpha\beta}\epsilon_{\gamma\alpha\beta}\sum_{i=1}^{N} l_{\alpha i,j}l_{\beta i,k}$ are constant coefficients, depending on the transf. matrix elements $l_{\alpha i,j}$ betw. the displacement coordinates $\Delta\alpha_i$ of the clusters wrt. the equilibrium positions α_i^e and the Q_j's in the body-fixed frame $i = 1, 2 \dots N$

- vibrational angular momentum operator: $p_\alpha = \sum_{jk=1}^{3N-6}\zeta^\alpha_{jk}Q_jP_k$ ⇝ P. Bunker and P. Jensen, *Fundamentals of Molecular Symmetry, CRC Press* (2004)
- rotational angular momentum operator, function of the *Euler angles* (χ, θ, φ):

$$J_x = -i\hbar\left\{\cos\varphi\left[\cot\theta\frac{\partial}{\partial\varphi} - \frac{1}{\sin\theta}\frac{\partial}{\partial\chi}\right] + \sin\varphi\frac{\partial}{\partial\theta}\right\} \quad J_y = -i\hbar\left\{\sin\varphi\left[\cot\theta\frac{\partial}{\partial\varphi} - \frac{1}{\sin\theta}\frac{\partial}{\partial\chi}\right] - \cos\varphi\frac{\partial}{\partial\theta}\right\} \quad J_z = i\hbar\frac{\partial}{\partial\varphi}$$

Remarks:

$\alpha, \beta, \gamma \dots = x, y, z \quad (\xi, \eta, \zeta)$ are the Cartesian components in the body-fixed or *instrinsic* (laboratory) frame
Anharmonic contrib. are not included in the potential, but may be relevant. Center-of-mass motion is neglected.

Approximation scheme for the Hamiltonian

- The construction of the *effective* reciprocal inertia tensor becomes increasingly difficult at growing N. Hence, it's convenient to operate a separation in the inertia tensor between the **static** part, $I^{\text{stat}}_{\alpha\beta}$, depending on the clusters equilibrium postions, $I^{\text{dyn}}_{\alpha\beta}$, and a **dynamic** part, depending on the Q_j's:

$$I_{\alpha\beta} \equiv I^{\text{stat}}_{\alpha\beta} + I^{\text{dyn}}_{\alpha\beta}$$

⇝ the separation is transferred to the *effective* inertia tensor

$$I^{\text{dyn},\zeta}_{\alpha\beta} \equiv I^{\text{dyn}}_{\alpha\beta} - \sum_{k=1}^{3N-6}\left(\sum_{j=1}^{3N-6}\zeta^{\alpha}_{jk}Q_j \sum_{l=1}^{3N-6}\zeta^{\beta}_{lk}Q_l\right)$$

Equipped with this separation, the *effective* reciprocal inertia tensor can be recast in Taylor series:

$$\boldsymbol{\mu} = (\mathbf{I}^{\text{stat}}+\mathbf{I}^{\text{dyn},\zeta})^{-1} = \left(\mathbb{1} - {\mathbf{I}^{\text{stat}}}^{-1}\mathbf{I}^{\text{dyn},\zeta} + {\mathbf{I}^{\text{stat}}}^{-1}\mathbf{I}^{\text{dyn},\zeta}{\mathbf{I}^{\text{stat}}}^{-1}\mathbf{I}^{\text{dyn},\zeta} + \dots\right){\mathbf{I}^{\text{stat}}}^{-1}$$

where $\mathbf{I}^{\text{dyn},\zeta}$ is treated as a «small» contribution. The *vibrational* angular momentum can be treated on the same footing. What springs from it is a systematic **approximation scheme** for the GαCM Hamiltonian:

$$H_{LO} = \frac{J^2}{2I^{\text{stat}}_{xx}} - \frac{J_z^2}{2}\left(\frac{1}{I^{\text{stat}}_{xx}} - \frac{1}{I^{\text{stat}}_{zz}}\right) + \frac{1}{2}\sum_{j=1}^{3N-6}P_j^2 + \frac{1}{2}\sum_{j=1}^{3N-6}\lambda_j^2Q_j^2 - \frac{\hbar^2}{8}\sum_{\alpha}\mu^{\text{stat}}_{\alpha\alpha}$$

$$H_{NLO} = H_{LO} - \frac{1}{2}\sum_{\alpha\beta}J_\alpha({I^{\text{stat}}_{\alpha\beta}}^{-1}I^{\text{dyn},\zeta}_{\beta\gamma}{I^{\text{stat}}_{\gamma\delta}}^{-1})J_\delta - \sum_{\alpha\beta}J_\alpha {I^{\text{stat}}_{\alpha\beta}}^{-1}p_\beta + \frac{\hbar^2}{8}\left({I^{\text{stat}}_{\alpha\beta}}^{-1}I^{\text{dyn},\zeta}_{\beta\gamma}{I^{\text{stat}}_{\gamma\alpha}}^{-1}\right)$$

$$H_{N^2LO} = H_{NLO} + \frac{1}{2}\sum_{\alpha\beta}p_\alpha({I^{\text{stat}}_{\alpha\beta}}^{-1})p_\beta + \frac{1}{2}\sum_{\alpha\beta}J_\alpha({I^{\text{stat}}_{\alpha\beta}}^{-1}I^{\text{dyn},\zeta}_{\beta\gamma}{I^{\text{stat}}_{\gamma\delta}}^{-1}I^{\text{dyn},\zeta}_{\delta\epsilon}{I^{\text{stat}}_{\epsilon\eta}}^{-1})J_\eta + \dots$$

H_{LO} corresponds to the **rigid rotor limit** for a *symmetric top*, in which rotations and vibrations are decoupled. Power counting is based on the number of p_α and $I^{\text{dyn},\zeta}_{\alpha\beta}$ insertions characterizing each contribution:

$$-\frac{1}{2}\sum_{\alpha\beta}J_\alpha({I^{\text{stat}}_{\alpha\beta}}^{-1}I^{\text{dyn},\zeta}_{\beta\gamma}{I^{\text{stat}}_{\gamma\delta}}^{-1}I^{\text{dyn},\zeta}_{\delta\epsilon}{I^{\text{stat}}_{\epsilon\eta}}^{-1})p_\eta \quad ⇝ \quad \text{order three} \quad \equiv N^3LO$$

Eigenvalues and pertubation theory

Fixing the axes of the body-fixed frame on the principal axes of inertia of the equilibrium α-cluster $\mathcal{D}_{4h}$ configuration, $I^{\text{stat}}_{\alpha\beta}$ is diagonal and the eigenvalues of the LO Hamiltonian are analytical:

$$E_{LO}(J,K,[\mathfrak{n}]) = \frac{\hbar^2}{2I^{\text{stat}}_{xx}}[J(J+1)-K^2]+\frac{\hbar^2}{2I^{\text{stat}}_{zz}}K^2+\sum_{i=1}^{6}\hbar\omega_i(\mathfrak{n}_i+\frac{1}{2})+\sum_{i=7}^{9}\hbar\omega_i(\mathfrak{n}_i+1)-\frac{\hbar^2}{8}\sum_{\alpha}I^{\text{stat}\,-1}_{\alpha\alpha}$$

where $\mathfrak{n}_i$ $\rightsquigarrow$ number of vibrational quanta of the mode i, vectorized as $[\mathfrak{n}]$

and $(\omega_1,\omega_2,\omega_3,\omega_4,\omega_5,\omega_6,\omega_7,\omega_7,\omega_8,\omega_8,\omega_9,\omega_9) \equiv (\lambda_1,\ \lambda_2\ \dots\ \lambda_{12})$ $\rightsquigarrow$ frequencies of the normal modes

and the modes $\omega_7,\omega_8,\omega_9$ are **doubly-degnerate**, whereas the others are 1-dimensional. The eigenvalues of H_{NLO} and higher-order Hamiltonians can be obtained only approximately, via perturbation theory (PT).

- Since $\mathbf{I}^{\text{dyn},\zeta}$ is non-diagonal, *triaxiality* emerges at a dynamical level in PT, although starting from an axially-symmetric rigid-rotor Hamiltonian at LO. Additionally, certain terms coupling $\mathbf{J}$ and $\mathbf{p}$ or $\mathbf{I}^{\text{dyn},\zeta}$ can be reproduced by means of Dunham expansion, $\rightsquigarrow$ L.J. Dunham, *Phys. Rev.* **41**, 721-731 (1932)

$$\Delta E_D([\mathfrak{n}],J) = \sum_{k=1}^{6}\sum_{ij} y_{ij}\left(\mathfrak{n}_k+\frac{1}{2}\right)^i[J(J+1)]^j+\sum_{k=7}^{9}\sum_{ij} y_{ij}(\mathfrak{n}_k+1)^i[J(J+1)]^j$$

where i, j are positive integers and y_{ij} are numerical coefficients.

- Anharmonicity, absent in this formulation of the GαCM Hamiltonian, can be modeled by adding on top of the rigid-rotor eigenvalues the correction in R. Bijker et al. *Nucl. Phys. A* **1006**, 122077 (2021) :

$$\Delta E_A([\mathfrak{n}]) = -\sum_{i=1}^{9}x_{ii}\mathfrak{n}_i+\sum_{i<j=1}^{9}x_{ij}\mathfrak{n}_i\mathfrak{n}_j$$

where x_{ij} are numerical coefficients.

The effect of anharmonicities can be assessed in states associated with multiple ($\mathfrak{n}_k \geq 2$) vibrational quanta. In ^{20}Ne, x_{ij} are small in negative-parity states and sizable (~ 1 MeV) and negative in positive-parity states.

Rotation-vibration eigenstates

- The eigenstates of the H_{LO} Hamiltonian are factorized into a rotational, $\psi_R^\pm$, and a vibrational part, ψ_V:

$$\Psi_{RV}^\pm \equiv \langle \mathbf{Q}, \mathbf{\Omega} | L^\pi M, \boldsymbol{\nu}\rangle \equiv \psi_R^\pm(\chi,\theta,\varphi)\psi_V(Q_1, Q_2 \dots Q_{3N-6})$$

Hermite polynomial

where $$\psi_V(Q_1, Q_2 \dots Q_{3N-6}) = \prod_{i=1}^{3N-6} \Phi_{\nu_i}(Q_i)$$ and $$\Phi_{\nu_i}(Q_i) = \sqrt{\frac{\omega_i}{2^{\nu_i}\nu_i!\hbar\sqrt{\pi}}} H_{\nu_i}\left(\sqrt{\frac{\omega_i}{\hbar}}Q_i\right)e^{-\frac{\omega_i}{2\hbar}Q_i^2}$$

are the one-dim. harmonic oscillator eigenfunctions. The excitation quanta «phonons» are encoded by

with $\nu_i = \mathfrak{n}_i$ for $i = 1, 2, \dots 6$ and $\nu_7 + \nu_8 = \mathfrak{n}_7$ $\nu_9 + \nu_{10} = \mathfrak{n}_8$ $\nu_{11} + \nu_{12} = \mathfrak{n}_9$

The latter are denoted also by the *irreducible representation* Γ according to which the normal coordinate Q_i transforms under the operations of $\mathcal{D}_{4h}$, the symmetry group of the equilibrium α-cluster configuration.

- The rotational states carry the parity $\pi = +$ and are expressed in terms of the Wigner D matrices, $D^J_{KM}(\chi,\theta,\varphi)$,

$$\psi_R^\pm(\chi,\theta,\varphi) \equiv \langle \chi,\theta,\varphi | J, M, K, \pm\rangle = \sqrt{\frac{(2J+1)}{16\pi^2(\delta_{K0}+1)}}\left[D^{J*}_{-KM}(\chi,\theta,\varphi) \pm (-1)^{J+K} D^{J*}_{KM}(\chi,\theta,\varphi)\right]$$

where
$J(J+1)\hbar^2 \rightsquigarrow$ eigenvalue of the total angular momentum operator $\mathbf{J}^2$
$M\hbar \rightsquigarrow$ eigenvalue of the projection $\mathbf{J}_z$ (body-fixed z-axis)
$K\hbar \rightsquigarrow$ eigenvalue of the projection $\mathbf{J}_\varsigma$ (laboratory-fixed z-axis)

Since the vibrational states have positive parity, the transformation properties of $\Psi_{RV}^\pm$ depend only on $\psi_R^\pm$. Starting from basis states of irreducible representations of SO(3), it is not possible to generate $J^\pi = 0^-$ states.

For the latter, one could resort to irreducible representations of O(3):

$\rightsquigarrow$ M.K.F. Wong, *J. Math. Phys.* **8**, 1899-1911 (1967)
M.K.F. Wong, *J. Math. Phys.* **10**, 1065-1068 (1969)

The role of symmetries

α-particles are stable bosonic (S = 0) and zero-isospin (T = 0) clusters of nucleons with mass $m \approx 3727.4$ MeV.

The LO GαCM Hamiltonian is invariant under parity, $\mathscr{P}$, time reversal, $\mathscr{T}$, the point group of the α-cluster configuration at equilibrium, $\mathcal{D}_{4h}$, as well as the full permutation-inversion group $\mathcal{G}(\mathrm{N}) \approx \mathcal{S}_6 \times \mathscr{P}$.

The *structure parameters* specifying the equilibrium α-configuration are β_1 and β_2.

By construction, the structure is axially –symmetric, hence SO(2)-invariant $\forall \beta_1,\ \beta_2$!

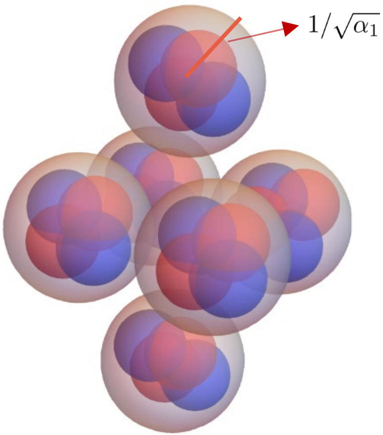

Representation with the adopted β_1 and β_2 and the underlying nucleons, having the experimental charge radii.

Adopted values:
$(\beta_1, \beta_2) = (2.38, 3.72)$ fm

Moments of inertia

pointlike charge dristribution:

$$I_{xx}^{\mathrm{stat}} = I_{yy}^{\mathrm{stat}} = 2m(\beta_1^2 + \beta_2^2)$$
$$I_{zz}^{\mathrm{stat}} = 4m\beta_1^2$$

Gaussian charge dristribution:

$$I_{xx}^{\mathrm{stat}} = I_{yy}^{\mathrm{stat}} = 2m(\beta_1^2 + \beta_2^2) + \frac{6m}{\alpha_1}$$
$$I_{zz}^{\mathrm{stat}} = 4m\beta_1^2 + \frac{6m}{\alpha_1}$$

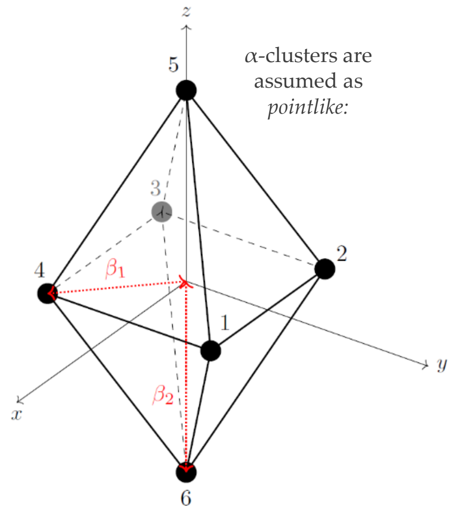

α-clusters are assumed as *pointlike:*

Experimental moments of inertia are nearer to the ones corresponding to a pointlike charge distribution.

R. Bijker et al., *Nucl. Phys. A* **1006**, 122077 (2021)

Transformation properties of the LO eigenstates

It is useful to consider the transformation properties under the operations of $\mathcal{D}_{4h}$ of the rotation-vibration states at LO, acting as reference states for the application of perturbation theory in the GαCM. The properties of the ψ_V's depend on the irreducible trepresentations according to which the normal coordinates transform.

Character table of $\mathcal{D}_{4h}$:

$\mathcal{D}_{4h}$	$\mathbb{I}$	$2C_4(z)$	C_2	$2C'_2$	$2C''_2$	i	$2S_4$	σ_h	$2\sigma_v$	$2\sigma_d$	Coordinates
A_{1g}	1	1	1	1	1	1	1	1	1	1	Q_1, Q_2
A_{2g}	1	1	1	-1	-1	1	1	1	-1	-1	
B_{1g}	1	-1	1	1	-1	1	-1	1	1	-1	Q_4
B_{2g}	1	-1	1	-1	1	1	-1	1	-1	1	Q_5
E_g	2	0	-2	0	0	2	0	-2	0	0	(Q_7, Q_8)
A_{1u}	1	1	1	1	1	-1	-1	-1	-1	-1	
A_{2u}	1	1	1	-1	-1	-1	-1	-1	1	1	Q_3
B_{1u}	1	-1	1	1	-1	-1	1	-1	-1	1	
B_{2u}	1	-1	1	-1	1	-1	1	-1	1	-1	Q_6
E_g	2	0	-2	0	0	-2	0	2	0	0	(Q_9, Q_{10}) (Q_{11}, Q_{12})

doubly-degenerate modes

Rules:

1. The HO eigenfunctions with zero vibration quanta transform as the A_g *irreducible representation* (irrep).

2. The HO eigenfunctions with one vibration quanta in the mode ω_i transform according to the same *irrep* as the normal coordinate Q_i.

3. The HO eigenfunctions with odd quanta in the non-degenerate mode ω_i ($i \leq 6$) transform as the normal coord. Q_i.

4. The HO eigenfunctions with even quanta in the non-degenerate mode ω_i ($i \leq 6$) transform the irrep A_g.

5. The HO eigenfunctions with $\mathfrak{n}_i$ quanta in the doubly-degenerate mode ω_i (i = 7,8,9) transform as the reducible representation whose characters are obtained from the symmetric $\mathfrak{n}_i$-th power of the irrep Γ_2 of the rel. coordinate pair:

$$\chi^{(\Gamma_2)^{\mathfrak{n}}}[R] = \frac{1}{2}\left\{\chi^{\Gamma_2}[R]\chi^{(\Gamma_2)^{\mathfrak{n}-1}}[R] + \chi^{\Gamma_2}[R^{\mathfrak{n}}]\right\} \qquad \forall R \in \mathcal{D}_{4h} \qquad \Gamma_2 = E_g, E_u$$

Transformation properties of the LO eigenstates

Summarizing, the transf. properties of the HO doubly-degenerate *vibrational eigenstates* are given by:

E_g: $\mathfrak{n}_7 =$	$\mathcal{D}_{4h}$
0	A_{1g}
1	E_g
2	$A_{1g} \oplus B_{1g} \oplus B_{2g}$
3	$2E_g$
4	$2A_{1g} \oplus A_{2g} \oplus B_{1g} \oplus B_{2g}$
5	$3E_g$
6	$2A_{1g} \oplus A_{2g} \oplus 2B_{1g} \oplus 2B_{2g}$

E_u: $\mathfrak{n}_8, \mathfrak{n}_9 =$	$\mathcal{D}_{4h}$
0	A_{1g}
1	E_u
2	$A_{1g} \oplus B_{1g} \oplus B_{2g}$
3	$2E_u$
4	$2A_{1g} \oplus A_{2g} \oplus B_{1g} \oplus B_{2g}$
5	$3E_u$
6	$2A_{1g} \oplus A_{2g} \oplus 2B_{1g} \oplus 2B_{2g}$

In a similar fashion, the analysis of the transformation properties of the *rotational states* (J ≤ 6), $\psi_R^{\pm}$ yields:

J^π	$\|K\|$	D_{4h}
0^+	0	A_{1g}
0^-	0	A_{1u}
1^+	0	A_{2g}
	1	E_g
1^-	0	A_{2u}
	1	E_u
2^+	0	A_{1g}
	1	E_g
	2	$B_{1g} \oplus B_{2g}$

J^π	$\|K\|$	D_{4h}
2^-	0	A_{1u}
	1	E_u
	2	$B_{1u} \oplus B_{2u}$
3^+	0	A_{2g}
	1	E_g
	2	$B_{1g} \oplus B_{2g}$
	3	E_g
3^-	0	A_{2u}
	1	E_u
	2	$B_{1u} \oplus B_{2u}$
	3	E_u

J^π	$\|K\|$	D_{4h}
4^+	0	A_{1g}
	1	E_g
	2	$B_{1g} \oplus B_{2g}$
	3	E_g
	4	$A_{1g} \oplus A_{2g}$
4^-	0	A_{1u}
	1	E_u
	2	$B_{1u} \oplus B_{2u}$
	3	E_u
	4	$A_{1u} \oplus A_{2u}$

J^π	$\|K\|$	D_{4h}
5^+	0	A_{2g}
	1	E_g
	2	$B_{1g} \oplus B_{2g}$
	3	E_g
	4	$A_{1g} \oplus A_{2g}$
	5	E_g
5^-	0	A_{2u}
	1	E_u
	2	$B_{1u} \oplus B_{2u}$
	3	E_u
	4	$A_{1u} \oplus A_{2u}$
	5	E_u

J^π	$\|K\|$	D_{4h}
6^+	0	A_{1g}
	1	E_g
	2	$B_{1g} \oplus B_{2g}$
	3	E_g
	4	$A_{1g} \oplus A_{2g}$
	5	E_g
	6	$B_{1g} \oplus B_{2g}$
6^-	0	A_{1u}
	1	E_u
	2	$B_{1u} \oplus B_{2u}$
	3	E_u
	4	$A_{1u} \oplus A_{2u}$
	5	E_u
	6	$B_{1u} \oplus B_{2u}$

EM multipole transition probabilities

- In the GαCM, the reduced electric or magnetic multipole transition probability between two rotation-vibration states with defined J^π nd K is defined as

$$B(R\lambda, J_i^{\pi_i}, |K_i|, [\mathfrak{n}]_i \to J_f^{\pi_f}, |K_f|, [\mathfrak{n}]_f) = \frac{1}{2J_i+1} \sum_{Mi=-J_i}^{J_i} \sum_{Mf=-J_f}^{J_f} \sum_{\mu=-\lambda}^{\lambda} |\langle J_f, M_f, |K_f|, [\mathfrak{n}]_f | \Omega_{\lambda\mu}(R) | J_i, M_i, |K_i|, [\mathfrak{n}]_i \rangle|^2$$

where the electric (R = E) and magnetic multipole (M) operators are defined in in the laboratory frame respectively. The intrinsic counterparts are linked to the lab. transition probabilities by a Wigner-D matrix:

$$\Omega_{\lambda\mu}(R) = \sum_{\nu=-\lambda}^{\lambda} D^{\lambda}_{\nu\mu}(\chi, \theta, \varphi)\ \omega_{\lambda\mu}(R)$$

- In the lab. frame , the $\Omega_{\lambda\mu}(E)$ transition operators transform as the A_{g} (A_{u}) irrep of $\mathcal{D}_{4h}$ when λ is even (odd). The opposite rule holds for $\Omega_{\lambda\mu}(M)$. Recalling the positions of the α-clusters in the laboratory frame, $\mathbf{R}_i \equiv (\xi_i, \eta_i, \zeta_i)$, the EM multipole transition operators can be written as:

$$\Omega_{\lambda\mu}(E) = \int \mathrm{d}^3 r\ r^\lambda Y_\lambda^\mu(\theta, \phi) \rho(\mathbf{r}) \qquad \Omega_{\lambda\mu}(M) = \int \mathrm{d}^3 r\ \mathbf{j}(\mathbf{r}) \cdot \mathbf{J} r^\lambda Y_\lambda^\mu(\theta, \phi)$$

where

$$\rho(\mathbf{r}) = e \sum_{i=1}^{Z} \delta(\mathbf{r} - \mathbf{R}_i) \quad \text{and} \quad \mathbf{j}(\mathbf{r}) = \frac{e\hbar}{2mi} \sum_{i=1}^{Z} [\delta(\mathbf{r} - \mathbf{R}_i) \overrightarrow{\nabla}_i - \overleftarrow{\nabla}_i \delta(\mathbf{r} - \mathbf{R}_i)]$$

are the *charge density* and the *current density* operators respectively.

Outlook:

The analysis of the transformation properties of $\omega_{\lambda\mu}(R)$ under $\mathcal{D}_{4h}$, together with the knowledge of the transformation properties of the reference H_{LO} eigenstates, and the *vanishing integral rule*, provides additional selection rules. In fact, the transition pattern itself is a fingerprint of $\mathcal{G}$!

⇝ G.S. et al., *J. of Phys. G* **43**, 085104 (2016)

Electric and magnetic moments

- The *electric quadrupole moment* is defined as the average value of $\Omega_{20}(E)$ calculated with respect to the state with maximum projection of J along the z axis of the laboratory frame, $M = J$:

$$Q(J^\pi, |K|, [\mathfrak{n}]) = \sqrt{\frac{16\pi}{5}} \langle J^\pi, |K|, J, [\mathfrak{n}] | \Omega_{20}(E) | J^\pi, |K|, J, [\mathfrak{n}] \rangle \equiv \frac{3K^2 - J(J+1)}{(2J+3)(J+1)} Q_0$$

for the 2_1^+ (1.369 MeV), the experimental *intrinsic* quadrupole moment, Q_0, is – 29.0(30) e fm^2

At LO in the GαCM with $(\beta_1, \beta_2) = (2.38, 3.72)$ fm and fitted values of the frequencies ω_i, one obtains:

$$Q_0 = -17.76 \text{ e fm}^2$$

From the intrinsic E2 moment, one obtains a classical constraint over the moments of inertia of the 6α system at equilibrium:

$$Q_0^{cl} = \frac{144\ m}{5} \left(\frac{1}{\mathscr{I}_z} - \frac{1}{\mathscr{I}_x} \right)$$

- Analogously, magnetic dipole moments are calculated on states with $M = J$:

$$\mu(J^\pi, |K|, [\mathfrak{n}]) = \sqrt{\frac{2\pi}{3}} \langle J^\pi, |K|, J, [\mathfrak{n}] | \Omega_{10}(M) | J^\pi, |K|, J, [\mathfrak{n}] \rangle$$

Calculations of the M1 moment are envisaged. Since the model does not account for the single-nucleon degrees of freedom, the most relevant contributions must come from the terms $\propto J_z$

$$\mu(J^\pi, |K|, [\mathfrak{n}]) \approx \frac{e\hbar^2}{2m} J$$

corresponding to a gyromagnetic factor of

$$g_\alpha \approx +0.5034$$

⇝ G.S. et al., *Eur. Phys. J.* **58**, 208 (2022)

- Due to the fact that proton and neutron degrees of freedom are absent in the GαCM, *electric dipole transitions* are zero in the model, at all orders in the approximation scheme, as they would entail a net displacement of the center-of-mass of the system.

Energy spectrum

Many of the observed energy levels lie between 10 and 13 MeV, many of them have uncertain J^π (red). Unambiguos lines are denoted in green.

Conventions:

1. The observed energy levels are classified into rotational bands, with definite K^π value.

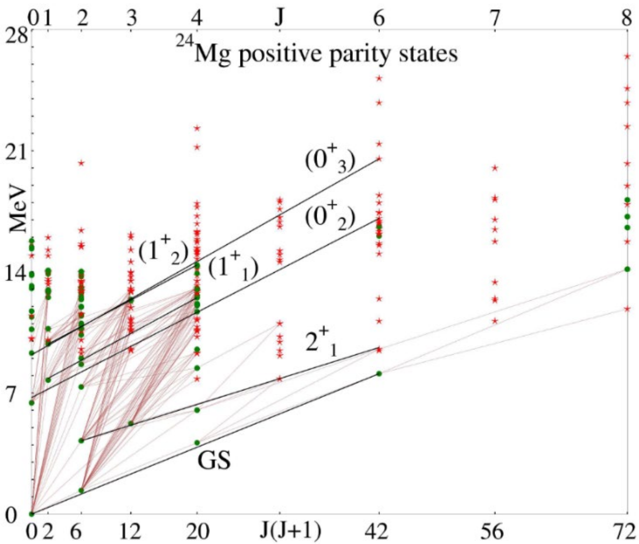

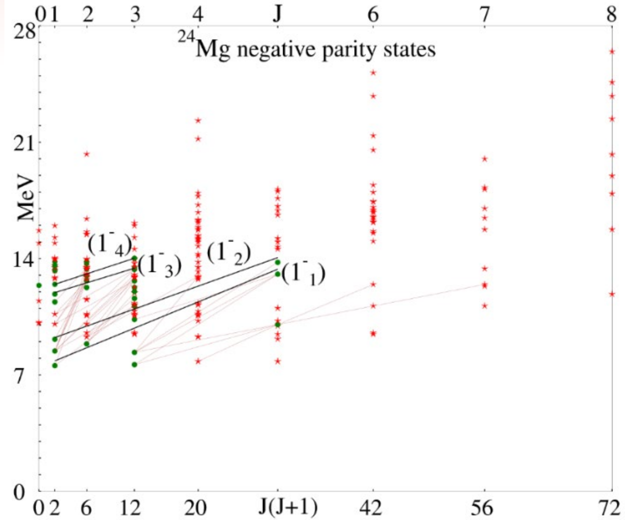

[J. Cseh. et al., *ArXiv:2312.08318 (2023)*]

In the GαCM framework

2. At LO, levels in the same band correspond to the same vibration eigenfunction, ψ_V.

3. As a consequence, bands are labeled by the irrep(s) of $\mathcal{D}_{4h}$ according to which the vibrational part of the eigenstates transform.

$\rightsquigarrow$ depends on the vib. quanta $[n]$!

Ground state band A_{1g}

- The states with zero quanta of vibration are distri-buted into two A_{1g} rotational bands: $K^\pi = 0^+$ and 4^+.

The classification of the $K^\pi = 0^+$ band agrees with NN-DC, and most theoretical investigations: J.D. Garrett *Phys. Rev. C.* **18**, 2032 (1978), L.K. Fifield et al. *Nucl. Phys. A* **322**, 1-12 (1979), J. Cseh et al. *Phys. Rev. C.* **48**, 1724 (1993), M. Kimura et al. *Prog. Theor. Phys.* **127**, 287, 2 (2012), J. Cseh et al. ArXiv:2312.08318 …

The exp. Q_0 indicates that ^{24}Mg is **prolate** in this band.

Nucleon-mass-specific moments of inertia: ⇝ $\mathscr{I}_x = 118.7(44)\ \text{fm}^2$, $\mathscr{I}_z = 41.7(20)\ \text{fm}^2$

- With the adopted (β_1 , β_2) values, the charge radius gives:

A_{1g} (g.s.) Band	Exper. fm	GαCM LO fm
$R_{ch}[0^+\ (0.0)]$	3.144	3.057(16)

and the reduced intraband E2 trans. probabilities (K^π=0^+) give:

Intraband A_{1g} (g.s.)	Experimental W.U.	Experimental $e^2\ fm^4$	GαCM LO $e^2\ fm^4$
B[$E2; 0^+\ (0.0) \to 2^+\ (1.369)$]	105.5^{+240}_{-230}	433.24^{+987}_{-946}	382.87
B[$E2; 2^+\ (1.369) \to 4^+\ (4.123)$]	50.0^{+47}_{-40}	205.5^{+196}_{-167}	196.90
B[$E2; 4^+\ (4.123) \to 6^+\ (8.113)$]	48.9^{+23}_{-13}	201.1^{+95}_{-53}	174.03
B[$E2; 6^+\ (8.113) \to 8^+\ (11.860)$]	n.a.	n.a.	164.93

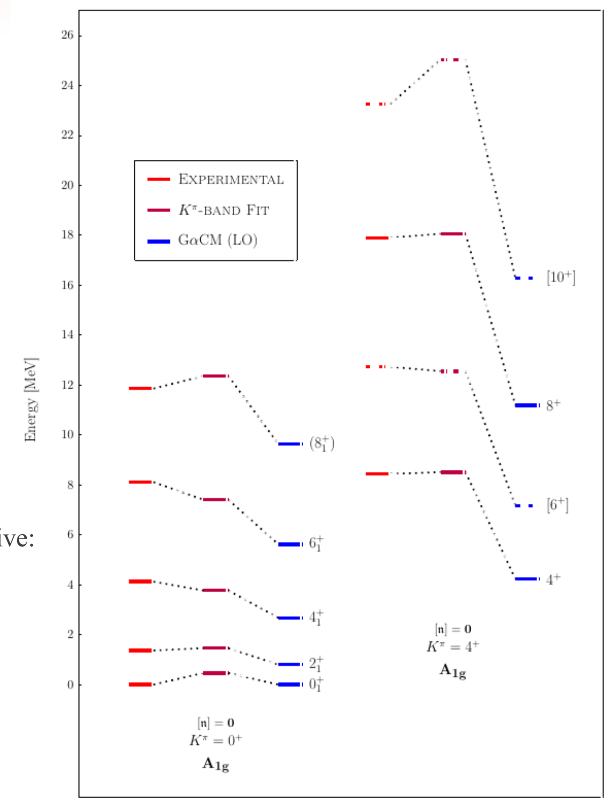

First excited band B_{2g}

- *Excitation quantum*: $\hbar\omega_5 = 2.997(29)$ MeV

associated with the normal coordinate:

$$Q_5 = \sqrt{m}\left(-\frac{\Delta x_1}{2\sqrt{2}} + \frac{\Delta x_2}{2\sqrt{2}} + \frac{\Delta x_3}{2\sqrt{3}} - \frac{\Delta x_4}{2\sqrt{3}} + \frac{\Delta y_1}{2\sqrt{2}} + \frac{\Delta y_2}{2\sqrt{2}} - \frac{\Delta y_3}{2\sqrt{2}} - \frac{\Delta y_4}{2\sqrt{2}}\right)$$

The $K^\pi = 2^+$ bandhead is a 2^+ at 4.123 MeV. The composition of the band reflects the literature assignments, corroborated by the NNDC. It is the most consolidated singly-excited band.

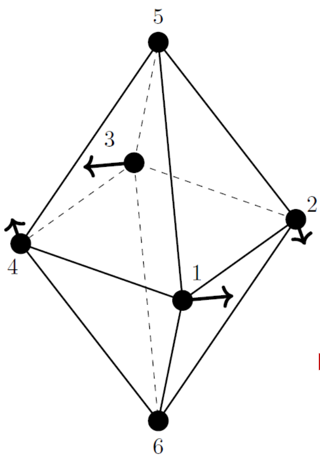

Q_5
ω_5

The 6^+ band is new and rather uncertain.

Nucleon mass-specific moments of inertia:

$$\mathscr{I}_x = 140.3(15)\ \mathrm{fm}^2$$
$$\mathscr{I}_z = 87.7(24)\ \mathrm{fm}^2$$

- **Description**: Symmetric *scissoring mode* of pairs of adjacent α-clusters in the xy plane. The basis of the bipyramid becomes rectangular. The apical α-clusters do not move.

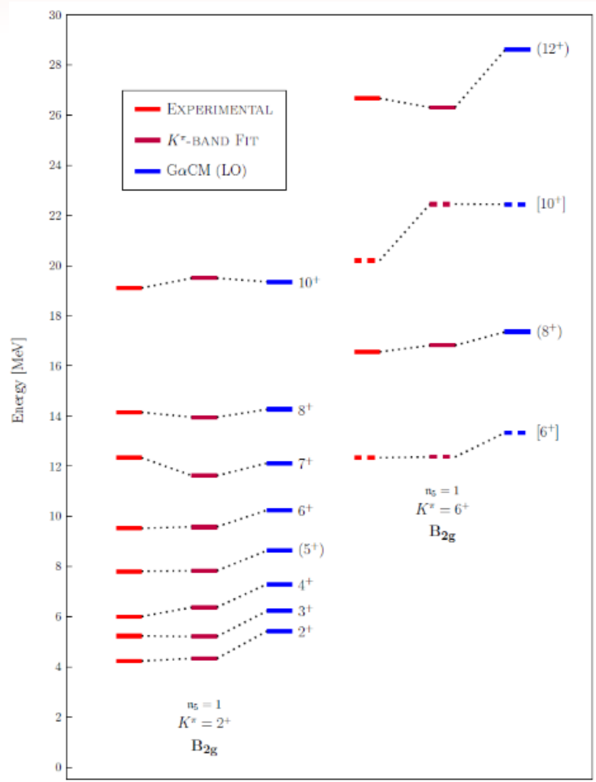

First excited band B_{2g}

- For the states belonging to this band, 2 *intraband* and 3 *interband* EM transitions have been measured.

Intraband B_{2g}	Experimental W.U.	Experimental e^2 fm^4	GαCM LO e^2 fm^4
$B[E2; 2^+ (4.123) \to 3^+ (5.235)]$	n.a.	n.a.	196.85
$B[E2; 2^+ (4.238) \to 4^+ (6.010)]$	26.82^{+216}_{-216}	110.30^{+888}_{-888}	84.36
$B[E2; 4^+ (6.010) \to 6^+ (9.528)]$	36.1^{+317}_{-130}	148.5^{+1307}_{-535}	133.62
$B[E2; 5^+ (7.812) \to 7^+ (12.340)]$	n.a.	n.a.	141.59
$B[E2; 6^+ (9.527) \to 8^+ (14.150)]$	n.a.	n.a.	146.02
$B[E2; 8^+ (14.150) \to 10^+ (19.110)]$	n.a.	n.a.	150.17

Nucleon-mass-specific moments of inertia:

$$\mathscr{I}_x = 140.3(15)\ \text{fm}^2$$
$$\mathscr{I}_z = 87.7(24)\ \text{fm}^2$$

- The calculated values of the reduced transition probabilities at LO in the GαCM agree with the experimental values within one standard deviation.

The slight deviations can be partly filled by GαCM at NLO in perturbation theory.

The predicted values not accompanied by the experimental counterpart could serve as possible 'α-cluster' benchmarks for the next measurements.

Interband $B_{2g} \leftrightarrow A_{1g} \oplus E_g\ (2\omega_5, \omega_7)$ (?)	Experimental W.U.	Experimental μ_N^2 fm^0	GαCM LO μ_N^2 fm^0
$B[M1; 2^+ (4.238) \to 2^+ (10.731)]$	$2.3^{+16}_{-7} \cdot 10^{-3}$	$4.12^{+290}_{-126} \cdot 10^{-3}$	$2.46 \cdot 10^{-3}$
$B[M1; 4^+ (6.010) \to 4^+ (n.a.)]$	n.a.	n.a.	$3.32 \cdot 10^{-3}$
$B[M1; 6^+ (9.528) \to 6^+ (n.a.)]$	n.a.	n.a.	$3.51 \cdot 10^{-3}$

Interband A_{1g} (g.s.) $\leftrightarrow B_{2g}$	Experimental W.U.	Experimental μ_N^2 fm^0	GαCM LO μ_N^2 fm^0
$B[M1; 2^+ (1.369) \to 2^+ (4.238)]$	$8.0^{+150}_{-40} \cdot 10^{-5}$	$14.3^{+267}_{-74} \cdot 10^{-6}$	0.0
$B[M1; 2^+ (1.369) \to 3^+ (5.235)]$	$4.26^{+301}_{-195} \cdot 10^{-5}$	$4.26^{+301}_{-195} \cdot 10^{-5}$	0.0

Work in progress:

The values in red correspond to incomplete calculations: more contributions are going to be summed up, after the correction of the M1 operator.

First excited band E_g

- *Excitation quantum*: $\hbar\omega_7 = 5.366(34)$ MeV

  associated with the normal coordinates:

$$Q_7 = \frac{\sqrt{m}}{\sqrt{\beta_1^2+\beta_2^2}}\left(\frac{\beta_2\Delta z_1}{2} - \frac{\beta_2\Delta z_2}{2} - \frac{\beta_2\Delta z_3}{2} + \frac{\beta_2\Delta z_4}{2} + \frac{\beta_1\Delta x_5}{\sqrt{2}} - \frac{\beta_1\Delta x_6}{\sqrt{2}}\right)$$

$$Q_8 = \frac{\sqrt{m}}{\sqrt{\beta_1^2+\beta_2^2}}\left(-\frac{\beta_2\Delta z_1}{2} - \frac{\beta_2\Delta z_2}{2} + \frac{\beta_2\Delta z_3}{2} + \frac{\beta_2\Delta z_4}{2} - \frac{\beta_1\Delta y_5}{\sqrt{2}} + \frac{\beta_1\Delta y_6}{\sqrt{2}}\right)$$

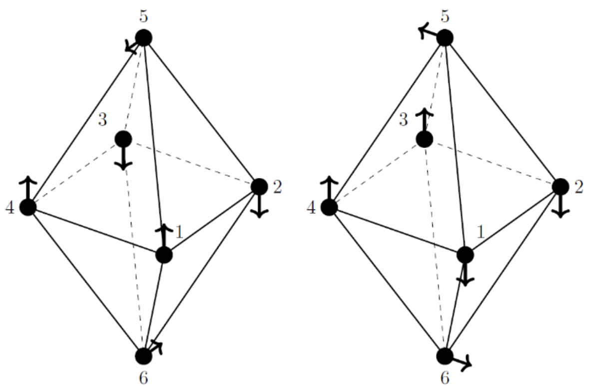

$\underset{\omega_7}{(Q_7, Q_8)}$

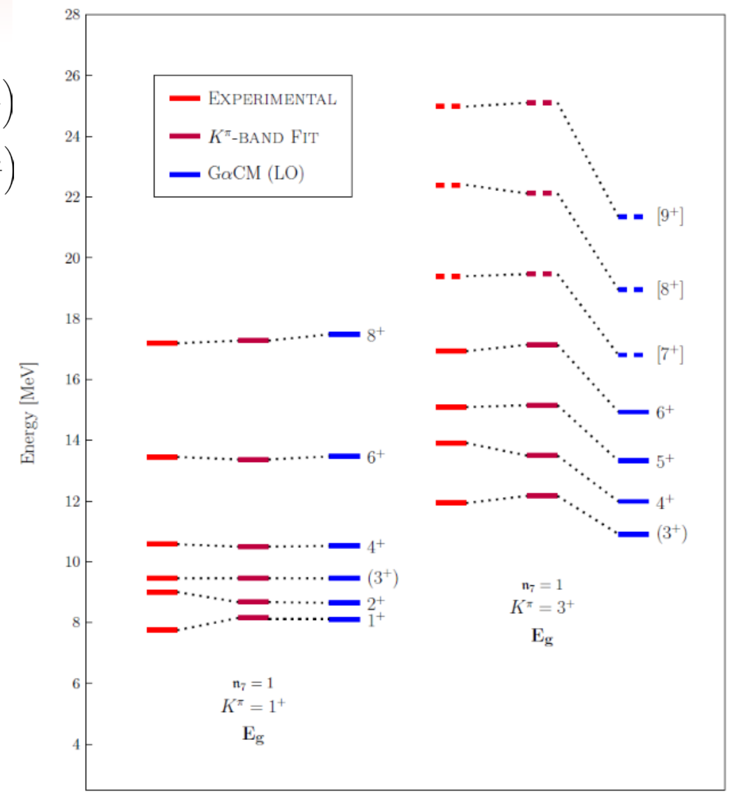

- **Description**: Asymmetric *twisting mode* of 3 adjacent α-clusters, one of them sitting in apical position. The dynamics favours the $^{12}C + {}^{12}C$ decay channel (13.934 MeV).

First excited band E_g

- The composition of the $K^\pi = 1^+$ band reflects entirely the assignments of Cseh (1993), Kimura (2012) and Cseh (2023). The $K^\pi = 3^+$ band agrees also with the predictions of the *algebraic $^{12}C + {}^{12}C$ cluster model* by Lévai (1993). This provides further support of the classification of this band as a E_g mode, whose dynamics enhances the formation of $^{12}C + {}^{12}C$ clusters. The fitted values of the moments of inertia for the two bands can be considered rather reliable.

Nucleon-mass-specific moments of inertia:

$$\mathscr{I}_x = 126.3(39)\ \mathrm{fm}^2$$

$$\mathscr{I}_z = 40.4(25)\ \mathrm{fm}^2$$

- The moment of inertia along the x axis shows a small increase with respect to the one of the g.s. band. The one along the z axis decreses moderately.

$\Downarrow$

Larger axial deformation!

Interband	Experimental		GαCM LO
$A_{1g}\ (\omega_2) \leftrightarrow E_g$	W.U.	$\mathrm{e}^2\ \mathrm{fm}^4$	$\mathrm{e}^2\ \mathrm{fm}^4$
$B[E2; 0^+\ (6.432) \to 2^+\ (9.004)]$	65.0^{+30}_{-25}	$\boxed{267.3^{+123}_{-103}}$	$\boxed{6.35 \cdot 10^{-2}}$
$B[E2; 2^+\ (8.654) \to 4^+\ (10.576)]$	n.a.	n.a.	$3.59 \cdot 10^{-2}$
$B[E2; 4^+\ (10.660) \to 4^+\ (10.576)]$	n.a.	n.a.	$1.63 \cdot 10^{-2}$

✗ Sharp disagreement with the GαCM predictions!

Interpretation: enhancement effect due to the vicinity of the 2+ at 8.655 MeV, whose transition strength to the 0+ at 6.432 MeV is comparable.

Mimicry mechanism? (M. Ploszajczak's talk on Tuesday)

Interband	Experimental		GαCM LO
$A_{1g}\ (g.s.) \leftrightarrow E_g$	W.U.	$\mathrm{e}^2\ \mathrm{fm}^4$	$\mathrm{e}^2\ \mathrm{fm}^4$
$B[E2; 0^+\ (0.0) \to 2^+\ (9.004)]$	0.860^{+170}_{-130}	3.54^{+70}_{-53}	18.68
$B[E2; 4^+\ (4.123) \to 2^+\ (9.004)]$	2.32^{+70}_{-61}	9.54^{+288}_{-251}	2.37

The E2 transition to the bandhead of the E_g band from the 0+ ground state is overestimated, whereas the opposite holds for the $4^+ \to 2^+$ transition between the A_{1g} (g.s.) and the E_g band.

First excited band $\mathrm{B_{1g}}$

- *Excitation quantum*: $\hbar\omega_4 = 6.141(55)$ MeV

associated with the normal coordinate: $Q_4 = \sqrt{m}\left(-\frac{\Delta x_1}{2\sqrt{2}} - \frac{\Delta x_2}{2\sqrt{2}} + \frac{\Delta x_3}{2\sqrt{3}} + \frac{\Delta x_4}{2\sqrt{3}} - \frac{\Delta y_1}{2\sqrt{2}} + \frac{\Delta y_2}{2\sqrt{2}} + \frac{\Delta y_3}{2\sqrt{2}} - \frac{\Delta y_4}{2\sqrt{2}}\right)$

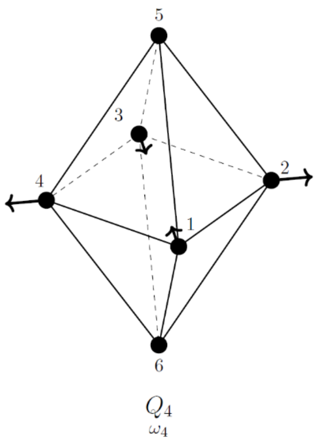

- **Description:** Asymmetric *stretching mode*, involving pairs of α-clusters sitting at the diagonal of the square in the xy plane. The apical α-clusters remain at rest.

- The composition of the $K^\pi{=}2^+$ band agrees with the considered literature, such as Cseh (1993), Cseh (2023). The 6^+ level, identified by Fifield (1979), is not recognized by the NNDC .

Mass-spec. moments of inertia:

$$\mathscr{I}_x = 132.9(58)\ \mathrm{fm}^2$$
$$\mathscr{I}_z = 92.6(44)\ \mathrm{fm}^2$$

- The calculated intraband transition probabilities are devoid of experimental counterpart.

Intraband B_{1g}	GαCM LO e^2 fm^4
$B[E2; 2^+\ (7.349) \to 3^+\ (9.533)]$	184.83
$B[E2; 2^+\ (7.349) \to 4^+\ (10.820)]$	79.21
$B[E2; 3^+\ (9.533) \to 4^+\ (10.820)]$	126.74
$B[E2; 4^+\ (10.820) \to 6^+\ (14.079)]$	125.46
$B[E2; 6^+\ (14.079) \to 8^+\ (18.16)]$	79.21

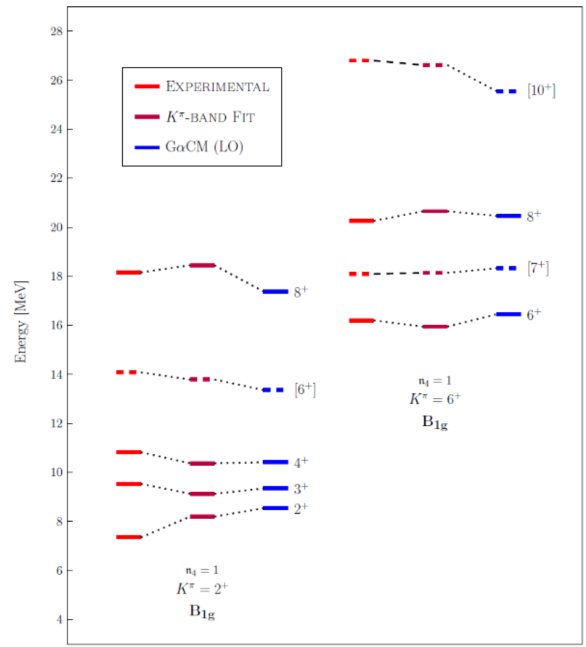

The $K^\pi{=}6^+$ band is among the least uncertain upper K-bands.

First excited band E_u

- *Excitation quantum*: $\hbar\omega_8 = 6.162(27)$ MeV

associated with the normal coordinates:

$$Q_9 = \sqrt{m}\left(-\frac{9\sqrt{3}}{2\sqrt{326}}\Delta x_1 + \frac{9\sqrt{3}}{2\sqrt{326}}\Delta x_2 - \frac{9\sqrt{3}}{2\sqrt{326}}\Delta x_3 + \frac{9\sqrt{3}}{2\sqrt{326}}\Delta x_4 + \frac{11\Delta y_1}{2\sqrt{978}} + \frac{11\Delta y_2}{2\sqrt{978}} + \frac{11\Delta y_3}{2\sqrt{978}} + \frac{11\Delta y_4}{2\sqrt{978}} - \frac{4\sqrt{2}}{\sqrt{489}}\Delta y_5 - \frac{4\sqrt{2}}{\sqrt{489}}\Delta y_6\right)$$

$$Q_{10} = \sqrt{m}\left(\frac{11\Delta x_1}{2\sqrt{978}} + \frac{11\Delta x_2}{2\sqrt{978}} + \frac{11\Delta x_3}{2\sqrt{978}} + \frac{11\Delta x_4}{2\sqrt{978}} - \frac{4\sqrt{2}}{\sqrt{489}}\Delta x_5 - \frac{4\sqrt{2}}{\sqrt{489}}\Delta x_6 - \frac{9\sqrt{3}}{2\sqrt{326}}\Delta y_1 + \frac{9\sqrt{3}}{2\sqrt{326}}\Delta y_2 - \frac{9\sqrt{3}}{2\sqrt{326}}\Delta y_3 + \frac{9\sqrt{3}}{2\sqrt{326}}\Delta y_4\right)$$

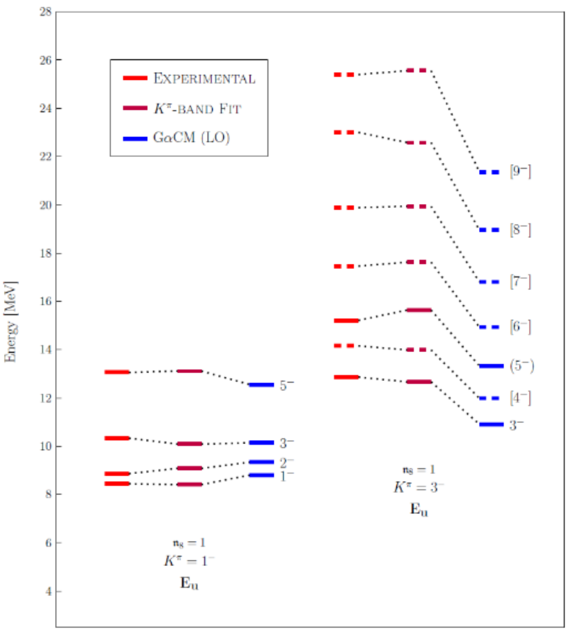

The composition of the $K^\pi = 1^-$ band agrees with Cseh (1993) and Cseh (2023), although lacks of high-J states.

- **Nucleon-mass-specific moments of inertia**:

$$\mathscr{I}_x = 125.3(28)\ \mathrm{fm}^2 \qquad \mathscr{I}_z = 42.6(21)\ \mathrm{fm}^2$$

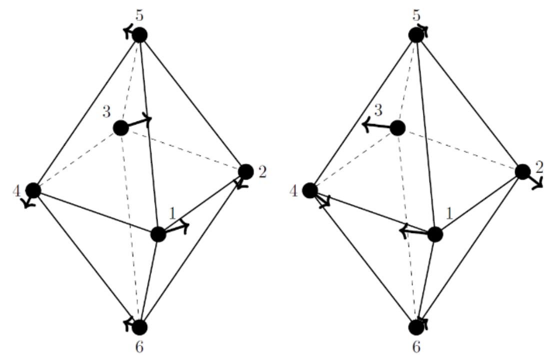

$\underset{\omega_8}{(Q_9, Q_{10})}$

- Description: Asymmetric *scissoring mode*, deforming the square in the xy plane into a trapezium. The apical α-clusters move in opposition to the shrinking edge of the square.

First excited band A_{1g}

- *Excitation quantum*: $\hbar\omega_2 = 6.4322(10)$ MeV
  associated with the normal coordinate:

$$Q_2 = \sqrt{m}\left(\frac{\Delta x_1}{2\sqrt{2}} - \frac{\Delta x_2}{2\sqrt{2}} - \frac{\Delta x_3}{2\sqrt{2}} + \frac{\Delta x_4}{2\sqrt{2}} + \frac{\Delta y_1}{2\sqrt{2}} + \frac{\Delta y_2}{2\sqrt{2}} - \frac{\Delta y_3}{2\sqrt{2}} - \frac{\Delta y_4}{2\sqrt{2}}\right)$$

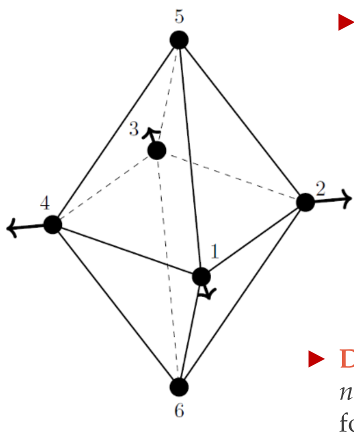

Q_2
ω_2

- The composition of the band partly agrees with the considered literature. The 4⁺ and 6⁺ lines differ from the ones in Cseh (1993).

Nucleon-mass-specific moments of inertia:

$$\mathscr{I}_x = 94.5(78)\ \mathrm{fm}^2$$
$$\mathscr{I}_z = \mathrm{n.a.}$$

- **Description**: Symmetric *stretching* or *planar breathing mode*, involving only the four α-clusters in the xy plane. The latter move along the diagonals of the square.

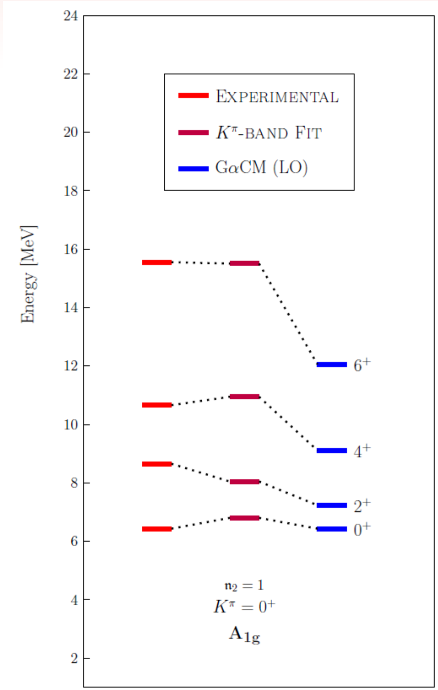

INTERBAND	EXPERIMENTAL		GαCM LO
A_{1g} $(g.s.) \leftrightarrow A_{1g}$ (ω_2)	fm^{-2} $[\rho(E0)^2]$	$\mathrm{e}^2\ \mathrm{fm}^0$	$\mathrm{e}^2\ \mathrm{fm}^0$
$\boxed{\mathrm{B}[E0; 0^+\ (0.0) \to 0^+\ (6.432)]}$	$370(70) \cdot 10^{-3}$	33.19^{+615}_{-615}	13.80

⇝ Measured electric **monopole** transition!

INTRABAND A_{1g} (ω_2)	EXPERIMENTAL		GαCM LO
	W.U.	$\mathrm{e}^2\ \mathrm{fm}^4$	$\mathrm{e}^2\ \mathrm{fm}^4$
$\mathrm{B}[E2; 0^+\ (6.432) \to 2^+\ (8.655)]$	45.0^{+160}_{-110}	185.1^{+658}_{-452}	369.43

Second excited band E_u

- *Excitation quantum*: $\hbar\omega_9 = 6.921(14)$ MeV

associated with the normal coordinates:

$$Q_{11} = \sqrt{m}\left(-\frac{5\Delta y_1}{2\sqrt{33}} - \frac{5\Delta y_2}{2\sqrt{33}} - \frac{5\Delta y_3}{2\sqrt{33}} - \frac{5\Delta y_4}{2\sqrt{33}} + \frac{2\Delta y_5}{\sqrt{33}} + \frac{2\Delta y_6}{\sqrt{33}}\right) \qquad Q_{12} = \sqrt{m}\left(-\frac{5\Delta x_1}{2\sqrt{33}} - \frac{5\Delta x_2}{2\sqrt{33}} - \frac{5\Delta x_3}{2\sqrt{33}} - \frac{5\Delta x_4}{2\sqrt{33}} + \frac{2\Delta x_5}{\sqrt{33}} + \frac{2\Delta x_6}{\sqrt{33}}\right)$$

The composition of the $K^\pi = 1^-$ band agrees with Cseh (1993), Cseh (2023), except for the 7^-, that has been added.

- **Nucleon-mass-specific moments of inertia**:

$$\rightsquigarrow \quad \mathscr{I}_x = 128.1(20)\ \mathrm{fm}^2 \qquad \mathscr{I}_z = 43.6(12)\ \mathrm{fm}^2$$

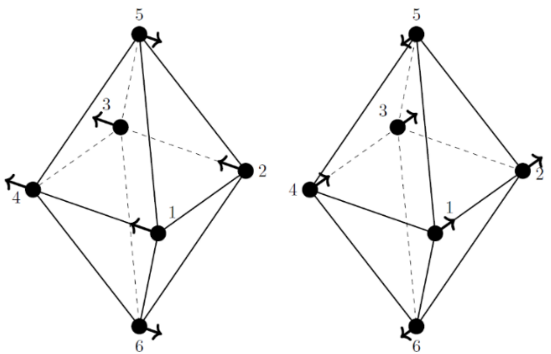

$\underset{\omega_9}{(Q_{11}, Q_{12})}$

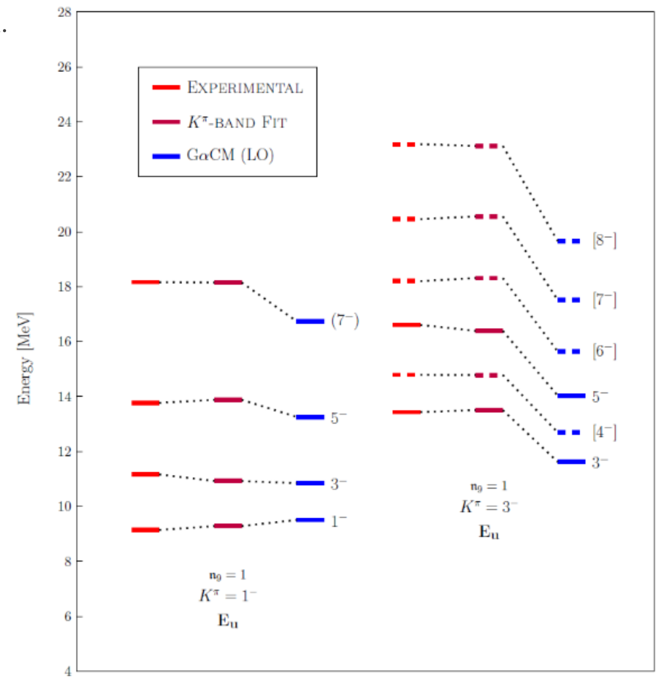

- **Description:** Asymmetric *rocking mode*, in which the planar α-clusters move in the same direction, parallel to the x or y axes, whereas the apical α-clusters displace in the same direction but opposite way.

First excited band A_{2u}

- *Excitation quantum*: $\hbar\omega_3 = 7.3722(10)$ MeV associated with the normal coordinate:

$$Q_3 = \sqrt{m}\left(-\frac{\Delta z_1}{2\sqrt{3}} - \frac{\Delta z_2}{2\sqrt{3}} - \frac{\Delta z_3}{2\sqrt{3}} - \frac{\Delta z_4}{2\sqrt{3}} + \frac{\Delta z_5}{\sqrt{3}} + \frac{\Delta z_6}{\sqrt{3}}\right)$$

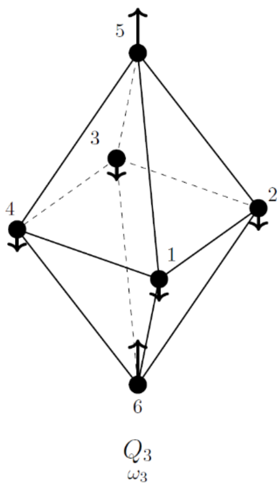

Nucleon-mass-specific moments of inertia:

$$\mathscr{I}_x = 226.5(52)\ \text{fm}^2$$

$$\mathscr{I}_z = 66.1(14)\ \text{fm}^2$$

- **Description**: Symmetric *wagging mode*, in which one apical α-cluster approaches the ones in the xy plane. The opposite apical cluster recedes from the xy plane, easing α + ^{20}Ne decay (threshold at 9.316 MeV).

- The K^π assignment of the 0^- band agrees with Garrett (1978), Cseh (1993), Kimura (2012), Kanada En'yo (2021) …

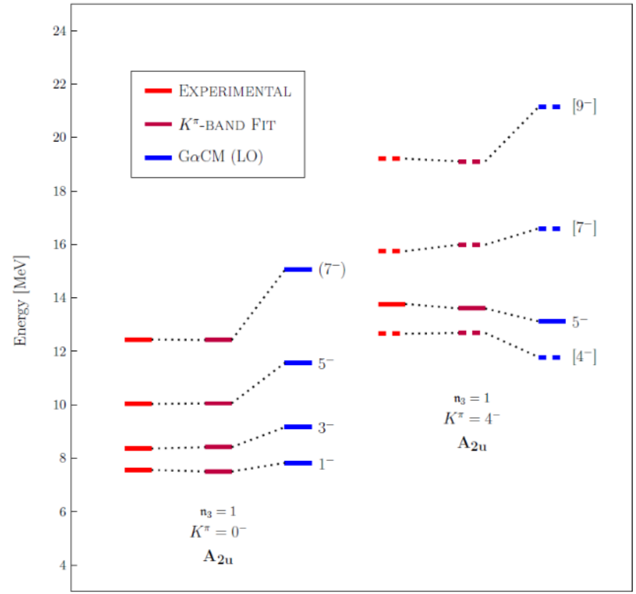

Interband A_{1g} (g.s.) $\leftrightarrow$ A_{2u}	Experimental W.U.	Experimental e^2 fm^6	GαCM LO e^2 fm^6
B[$E3; 0^+$ (0.0) $\to 3^-$ (8.358)]	72.8^{+140}_{-119}	2491^{+479}_{-407}	1396.24
B[$E3; 2^+$ (1.369) $\to 5^-$ (10.028)]	85.8^{+396}_{-242}	2936^{+1355}_{-828}	664.88

Intraband A_{2u}	Experimental W.U.	Experimental e^2 fm^4	GαCM LO e^2 fm^4
B[$E2; 3^-$ (8.358) $\to 5^-$ (10.028)]	50.29^{+220}_{-126}	206.8^{+518}_{-518}	178.18

Second excited band A_{1g}

- *Excitation quantum*: $\hbar\omega_1 = 9.30539(24)$ MeV associated with the normal coordinate:

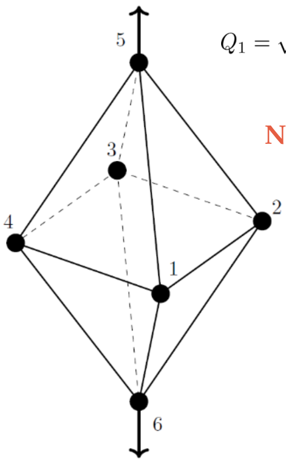

Q_1
ω_1

$$Q_1 = \sqrt{m}\left(\frac{\Delta z_5}{\sqrt{2}} - \frac{\Delta z_6}{\sqrt{2}}\right)$$

Nucleon-mass-specific moments of inertia:

$$\mathscr{I}_x = 156.3(159)\ \text{fm}^2$$
$$\mathscr{I}_z = \text{n.a.}$$

- **Description:** Symmetric *stretching* or *axial breathing mode*, involving only the two apical α-clusters. The mode enhances the $2\alpha+^{16}O$ configura-tion (threshold at 14.047 MeV).

- No M1 or E2 transition probabilities have been measured between the states of this band.

Interband $A_{1g}\ (g.s.) \leftrightarrow A_{1g}\ (\omega_1)$	GαCM LO $e^2\ \text{fm}^{2\lambda}$
$B[E0; 0^+\ (0.0) \to 0^+\ (9.305)]$	16.86
$B[E2; 0^+\ (0.0) \to 2^+\ (10.660)]$	24.73

- The composition of this band is less certain the one of all the other singly-excited rotational bands. This is also due to the large amount of 2^+ and 4^+ levels popolating the 10-13 MeV region.

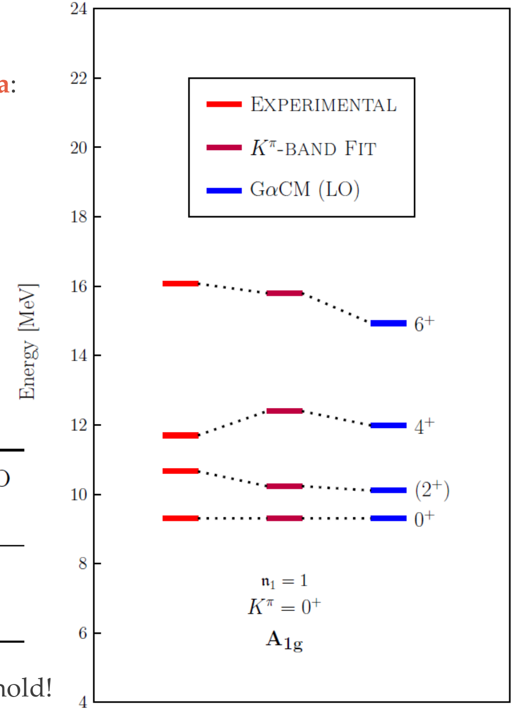

NB: The 0^+ bandhead is just below (< 0.1 MeV) the $\alpha + ^{20}Ne$ decay threshold!

First excited band B_{2u}

- **Excitation quantum:** $\hbar\omega_6 = 10.721(71)$ MeV associated with the normal coordinate:

$$Q_6 = \sqrt{m}\left(\frac{\Delta z_1}{2} - \frac{\Delta z_2}{2} + \frac{\Delta z_3}{2} - \frac{\Delta z_4}{2}\right)$$

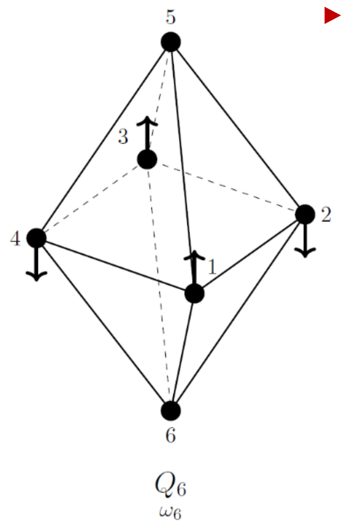

- The composition of the whole singly-excited B_{2u} band represents an original work. The 2^- bandhead is rarely cited in the considered references. In Cseh (1993) is taken as a part of a 1^- band.

Nucleon-mass-specific moments of inertia:

$$\mathscr{I}_x = 133.5(69)\ \text{fm}^2$$
$$\mathscr{I}_z = 67.5(32)\ \text{fm}^2$$

No experimental intraband transition probabilities are available!

- **Description:** Symmetric *twisting mode*, in which pairs of planar α-clusters sitting along the diagonal of the square move in the axial direction, in the opposite way. The apical clusters remain at rest.

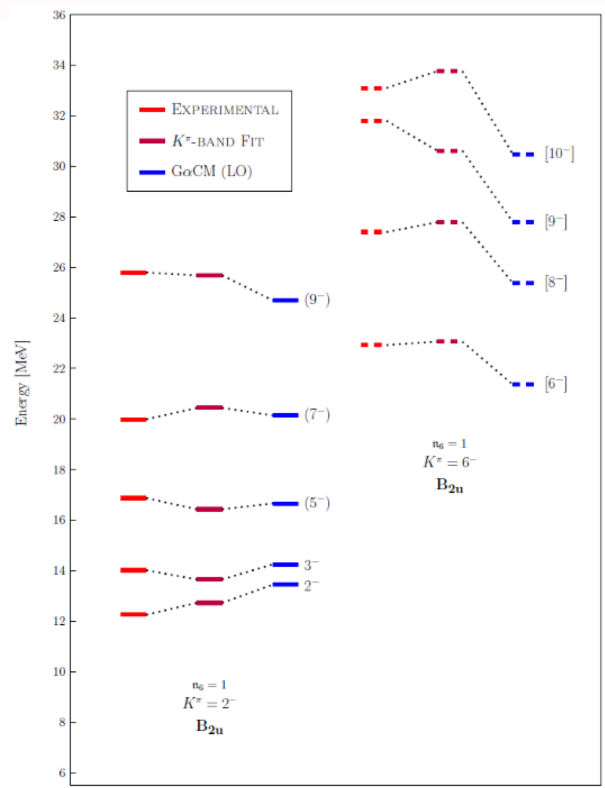

Conclusion

- Motivated by the recent application of a macroscopic model with $\mathcal{D}_{3h}$ symmetry on ^{20}Ne we have:

✓ defined an approximation scheme which couples rotational with vibrational motion for the systematic improvement of the rigid rotor Hamiltonian for α-conjugate nuclei;

✓ tested the $\mathcal{D}_{4h}$ symmetric square bipyramid as an equilibrium α-cluster configuration for the GαCM applied to the ^{24}Mg, identifying all the 9 singly-excited rotational bands, of which the two excited A_{1g} bands are made partially of new assignments, whereas the B_{2u} is totally new;

✓ The composition of the $K^\pi = 3^\pm$, $4^\pm$ and $6^\pm$ *singly-excited rotational* bands – except for the E_g case - is quite speculative, due also to the uncertain J^π assignment of part of the observed energy levels;

✓ calculated a sample of intraband and interband reduced EM multipole transition probabilities between the identified α-cluster states of ^{24}Mg, finding in most cases reasonable agreement with experimental data;

✓ highlighted the connection between certain normal modes (A_{1g}, A_{2u}, E_g) and the principal α-decay channels.

Outlook:

✓ Fitting of the structure parameters (β_1 , β_2) based on the inelastic form factor $F^2(q; 0_1^+ \to 0_2^+)$, similarly to ref. R. Bijker et al. , *Nucl. Phys. A* **1006**, 122077 (2021);

✓ Correction of the M1 transition operator and prediction of the measured M1 and M2 transitions;

✓ Perturbative application of the NLO rotation-vibration coupling, at least to a small sample of excitations;

✓ Tentative inspection of doubly-excited rotational bands, with special attention to neighbour states of α-decay thresholds at 13.934 MeV (^{12}C + ^{12}C), 14.047 MeV(2α+^{16}O) and 21.21 MeV (3α+^{12}C).

Acknowledgements:

D. Lee (Michigan State Univ.), **K.H. Speidel** (HISKP Bonn, *in memoriam*) and **V. Somà** (CEA Paris-Saclay)

Thank you for the attention!

Enjoy the rest of the workshop!

«Light Nuclei between single-particle and clustering features»

3rd-6th December 2024

Light Nuclei Workshop
CEA Paris-Saclay
2024

Commissariat à l’Énergie Atomique et aux Énergies Alternatives - www.cea.fr

Irrelevant energy levels

As for other α-conjugate nuclei, not all the observed energy levels can fit the GαCM framework.

- Among the **T = 0** and unlabeled lines, the following do not fit $\mathcal{D}_{4h}$ symmetry or do not exhibit α-clustering:

J^π	Energy [MeV]	J^π	Energy [MeV]	J^π	Energy [MeV]
$n.a.$	7.000	$(2^+, 4^+)$	9.284	(5^-)	11.909
3^-	7.616	$n.a.$	9.300	$n.a.$	14.793
(5^-)	9.160	$(5^-, 6^+)$	9.450	$n.a.$	15.093

- In addition, levels with uncertain isospin assignment (**T = 0,1**) could be neglected:

J^π	Energy [MeV]	J^π	Energy [MeV]	J^π	Energy [MeV]
1^+	9.828	$(2^+, 3^-, 4^+)$	12.921	3^-	13.346

- Finally, levels with **T = 1** do not represent α-cluster energy levels, hence must be discarded:

J^π	Energy [MeV]	J^π	Energy [MeV]	J^π	Energy [MeV]
4^+	9.516	2^+	12.405	$(2^+, 3^-)$	13.030
$n.a.$	9.965	1^+	12.527	4^+	13.050
$(1^+, 2^+)$	10.059	4^+	12.639	2^+	13.089
1^+	10.712	2^-	12.670	$(2^\pm)$	13.367
$(3^\pm, 5^+)$	11.012	1^+	12.8181	(6^-)	15.045
4^+	12.051	1^+	12.955	–	–

Work in progress: Further levels of the experimental ^{24}Mg spectrum could be set apart when the analysis of the double vibrational excitations will be carried out.